Structured Cyclic Peptides That Bind the EH Domain of EHD1

Alissa J. Kamens,[†] Robyn J. Eisert,[†] Tiffany Corlin,[‡] James D. Baleja,[‡] and Joshua A. Kritzer*,[†]

[†]Department of Chemistry, Tufts University, 62 Talbot Avenue, Medford, Massachusetts 02155, United States
[‡]Department of Developmental, Molecular, and Chemical Biology, Tufts University School of Medicine, 136 Harrison Avenue, Boston, Massachusetts 02111, United States

Ⓢ *Supporting Information*

ABSTRACT: EHD1 mediates long-loop recycling of many receptors by forming signaling complexes using its EH domain. We report the design and optimization of cyclic peptides as ligands for the EH domain of EHD1. We demonstrate that the improved affinity from cyclization allows fluorescence-based screening applications for EH domain inhibitors. The cyclic peptide is also unusually well-structured in aqueous solution, as demonstrated using nuclear magnetic resonance-based structural models. Because few EH domain inhibitors have been described, these more potent inhibitors will improve our understanding of the roles of EHD1 in the context of cancer invasion and metastasis.

The dysregulation of endocytosis and vesicle trafficking is a characteristic feature of many cancers, particularly during the poorly understood processes of invasion and metastasis.[1] Critical receptors responsible for cell signaling, cell−cell interactions, and cell−matrix interactions all require endocytosis and recycling pathways for their roles in malignant growth. For example, an increase in the long-loop recycling of $\beta 1$-integrins is observed in motile cancer cells, assisting polarization and invasion.[1,2] Thus, the proteins involved in the long-loop recycling pathway are potential anti-invasiveness cancer targets. While some chemical tools for modulating vesicle trafficking are available, no specific inhibitors of long-loop recycling have been discovered to date.[3−5] EH domain-containing protein 1 (EHD1) has emerged as a critical regulator of long-loop endocytic recycling. Genetic knockdown of EHD1 prevents recycling of $\beta 1$-integrin, and misregulation and mutation of EHD1 have been implicated in cancer progression.[6,7]

EHD1 binds several key proteins involved in vesicle trafficking, many via its EH domain. Proteins with C-terminal EH domains, such as EHD1, are primarily involved in intracellular vesicular transport, while proteins with N-terminal EH domains, such as Eps15, are more involved in endocytosis.[6,8] These two functional classes of EH domains also have different substrate preferences, but all EH domains recognize a core asparagine-proline-phenylalanine (NPF) motif. Nuclear magnetic resonance (NMR) structures of NPF-containing peptides bound to EH domains, including the EH domain of EHD1, have revealed that the NPF motif forms a type 1 β-turn when bound.[9−11]

Previous attempts to identify binding partners of EH domains have used yeast two-hybrid screens, phage-display selections, and pull-down assays.[12−15] However, all identified inhibitors to date are linear peptides with low affinities. Using isothermal titration calorimetry (ITC), we measured the affinity (K_d) of a typical linear peptide ligand to be 35.7 ± 3.7 μM at 20 °C and a physiological salt concentration (Table S2 of the Supporting Information). To date, quantitative determination of peptide−EH domain affinities relied on NMR and ITC, which are robust but demanding assays, and typically required low-salt or no-salt conditions to increase affinity (Table S2 of the Supporting Information). Without higher-affinity inhibitors, practical assays with higher throughput and a low level of reagent consumption (such as fluorescence polarization) have not been feasible.

Earlier work with linear peptides established that C-terminal type EH domains prefer multiple negatively charged residues directly C-terminal to the NPF motif.[16,17] Thus, we incorporated the sequence NPFEE within a head-to-tail cyclic peptide, with the hypothesis that cyclization would stabilize the β-turn and preorganize the binding epitope.[17] A tyrosine was also included N-terminal to the NPF sequence because it is present in endogenous EHD1-EH ligands and allowed for spectrophotometric determination of the ligand concentration. For direct comparison to prior work in this area, we first analyzed ligand binding to EHD1-EH by ITC with no NaCl and then repeated the experiments at 15 and 150 mM NaCl (Table S2 and Figure S3 of the Supporting Information). At physiological NaCl concentrations, cyclic peptide cNPF1 had a K_d of 9.9 ± 0.8 μM. The nearly 4-fold improvement in affinity was consistent at all salt conditions. This suggested that the increase in affinity was not due to electrostatic interactions, but rather the conformation of the NPF motif. These data indicated that the NPF motif and flanking residues were able to make more favorable contacts with EHD1-EH within the context of a cyclic scaffold.

While ITC is powerful, we sought a more rapid and convenient assay for discovering EHD1-EH inhibitors. To this end, we linked cNPF1 to fluorescein (cNPF1^{Flu}) to monitor direct EHD1-EH binding using fluorescence polarization (FP). We also synthesized dye-labeled cNPF1 analogues with an altered ring size (cNPF2^{Flu} and cNPF3^{Flu}), cNPF1 analogues with a reduced overall negative charge (cNPF4^{Flu} and cNPF5^{Flu}), and linear and non-NPF-containing controls (sequences listed in Table 1). FP assays were performed at

Table 1. Binding of Dye-Labeled Probes to EHD1-EH

peptide	sequence	K_d $(\mu M)^a$	low-salt K_d $(\mu M)^b$
Lin^{Flu}	^{Flu}-$\beta\beta$YNPFEE-$_{NH2}$	31.4 ± 0.5	6.9 ± 0.6
cNPF1^{Flu}	-YNPFEEGK(Flu)-	16.8 ± 0.1	3.3 ± 0.3
cNPF2^{Flu}	-YNPFEEγK(Flu)-	20.5 ± 0.3	4.5 ± 0.3
cNPF3^{Flu}	-YNPFEEK(Flu)-	57.8 ± 0.2	11.3 ± 1.0
cNPF4^{Flu}	-YNPFAEGK(Flu)-	46.7 ± 0.9	17.4 ± 0.1
cNPF5^{Flu}	-YNPFEAGK(Flu)-	28.3 ± 0.3	8.7 ± 0.9
cNPF6^{Flu}	-YNPFEQGK(Flu)-	34.0 ± 0.3	12.8 ± 0.8
cAPA^{Flu}	-YAPAEEGK(Flu)-	nd^c	>67

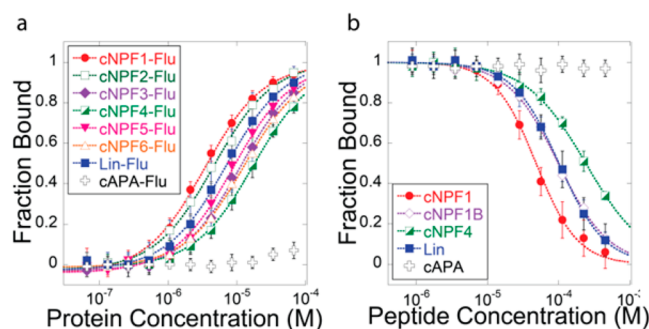$^a K_d$ at 150 mM NaCl. $^b K_d$ at 15 mM NaCl. ^{c}Not determined.

Figure 1. (a) Direct binding assay of each probe with EHD1-EH. Curve fits match the K_d values reported in Table 1. (b) Competitive binding assay with cNPF1^{Flu}. Curve fits match the IC$_{50}$ values reported in Table 2. Error bars show the standard deviation from three or more independent trials. Experiments were performed in 25 mM MOPS (pH 6.8), 1 mM CaCl$_2$, and 15 mM NaCl with 1.5% DMSO and 0.1% Tween 20.

15 and 150 mM NaCl (Figure 1a, Figure S4 of the Supporting Information, and Table 1). At 15 mM NaCl, the data fit well to a two-state binding curve. Reduced affinities were observed at 150 mM NaCl, but these data were fit well by assuming upper bounds for polarization similar to those observed at 15 mM (Figure S4 of the Supporting Information). The FP assay produced K_d values similar to those obtained by ITC, with very similar trends among linear and cyclic peptides, and among different salt concentrations. We concluded that this FP assay was reliable for assessing binding to EHD1-EH. We also showed that increasing the ring size (cNPF2^{Flu}) or decreasing the ring size (cNPF3^{Flu}) within cNPF1^{Flu} led to poorer binding. This is consistent with the hypothesis that a specific cyclic structure improves binding of the NPFEE sequence to EHD1-EH.

To rule out the possibility that nonspecific electrostatics dominates cNPF1 binding, we tested a cyclic peptide that maintained the negative charge but lacked the critical NPF motif (cAPA^{Flu}). No binding was observed up to 67 μM EHD1-EH even at 15 mM NaCl, demonstrating that an intact NPF motif is the primary requirement for binding. Next, we probed the effects of reducing the number of charged residues in the context of a cyclic peptide with cNPF4^{Flu}, cNPF5^{Flu}, and cNPF6^{Flu}. All three of these inhibitors had less affinity for EHD1-EH, which demonstrated that negatively charged flanking sequences boost affinity for cyclic ligands, as they do for linear ligands.[16,17] Interestingly, cNPF5^{Flu} exhibited an only 3-fold loss of affinity. This implies that EHD1-EH ligands with moderate affinity and reduced negative charge can be further designed and optimized, either as a free acid or in an esterified form, for later cellular studies.

To evaluate the selectivity of our probes for EHD1-EH over unrelated EH domains, we expressed and purified the second EH domain of Eps15 (Eps15-EH2) and used circular dichroism spectroscopy to verify that it was properly folded (Figure S5b of the Supporting Information).[16] Under low-salt conditions, the dye-labeled probes were unable to bind this EH domain up to an Eps15-EH2 concentration of 50 μM (Figure S4d of the Supporting Information). This provided initial evidence that these probes are selective for the C-terminal type of EH domain (EHD1-EH) over the N-terminal type of EH domain (Eps15-EH2).

To develop an assay suitable for high-throughput screening applications, we used cNPF1^{Flu} to set up a FP competitive binding assay. The probe was used with a range of inhibitors to establish its effectiveness for future screens (Figure 1b and Table 2). As with the direct binding assays, cNPF1 was the

Table 2. Competition Assay for EHD1-EH Binding

peptide	sequence	IC$_{50}$ (μM)
linear	^{Ac}-YNPFEEGG-$_{NH_2}$	107 ± 1
cNPF1	-YNPFEEGG-	49.2 ± 0.2
cNPF1B	-YNPFEEGK(Ac)-	100 ± 1
cNPF4	-YNPFAEGG-	240 ± 1
cAPA	-YAPAEEGG-	>450

strongest inhibitor. An analogue of cNPF1^{Flu} with an acetyl group in place of the dye was also tested and showed 2-fold less potent inhibition (Table 2). This suggests that the introduction of the dye decreases the cNPF1 affinity and that its positioning within the cNPF1 ring could be further optimized. cNPF4 was tested as an example of a lower-affinity inhibitor, and cAPA was used as a negative control. Because the results showed the same trends observed in direct binding assays, we concluded that this competitive binding assay represents a useful assay for high-throughput screening for EH domain inhibitors.

As a complement to screening, we also sought a basis for the structure-based design of additional macrocyclic EH domain inhibitors. We determined the solution structures of the linear NPF-containing peptide and the cyclic peptide cNPF1 (Figure 2). The linear peptide was relatively unstructured in aqueous solution (Figure 2a), though some low-energy conformations showed the characteristic β-turn. cNPF1, by contrast, adopted a tight ensemble of well-structured conformations in aqueous solution (Figure 2b). This is unusual for a cyclic octamer, and the surprising degree of structure is likely promoted by the turn-forming NPF sequence. The NPF motif of cNPF1 formed a β-turn in solution that was nearly identical to the turn observed in linear NPF motifs bound to EHD1-EH.[17] When superimposed with the NPF motif within a previously determined NPF/EHD1-EH structure, the backbone of cNPF1 overlaid with the NPFE sequence of the ligand with a root-mean-square deviation of 0.333 Å (Figure 2c). A posed model of cNPF1 within the binding site of EHD1-EH (Figure 2d) provides a clear rationale for the observed structure–activity relationships within cNPF1 analogues and provides an excellent starting point for the structure-based design of additional cyclic peptide and small-molecule macrocycle inhibitors of EHD1-EH.[17]

There are relatively few chemical agents that can be used to study vesicle trafficking, and even molecules with relatively high IC$_{50}$ values are welcomed as useful tools. For example, the small molecule dynasore, first reported in 2006, has an IC$_{50}$ of ∼15
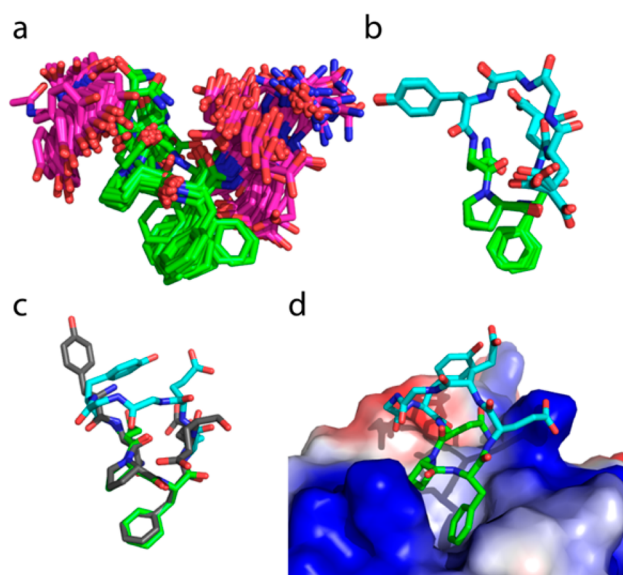
Figure 2. (a) Thirty lowest-energy structures calculated for the linear NPF-containing peptide (Ac-YNPFEEGG-NH$_2$ sequence) in aqueous solution. The NPF motif is colored green, and other residues are colored magenta. (b) Thirty lowest-energy structures calculated for cNPF1 in aqueous solution. The NPF motif is colored green, and other residues are colored cyan. (c) Overlay of cNPF1 with the structure of the YNPFEE sequence from a peptide bound to EHD1-EH. The backbone overlay for the residues NPFE has a root-mean-square deviation of 0.333 Å. cNPF1 is colored as in panel b, and YNPFEE is colored gray. (d) Solution structure of cNPF1 positioned in the binding pocket of EHD1-EH. cNPF1 is colored as in panel b, and EHD1-EH is shown as a surface colored according to electrostatics.

μM in a biochemical assay of dynamin GTPase activity.[18] It is widely used to study clathrin-dependent endocytosis despite the fact that it is typically applied at a concentration of 80 μM.[19] By this standard, cNPF1 and related molecules have potential as chemical biology tools, pending further work to maximize target affinity and cell penetration. The 4-fold improvement in affinity for cNPF1 over those of linear peptides also allowed the development of a straightforward fluorescence polarization competition assay. This assay is high-throughput-ready and will accelerate the development of additional classes of constrained peptides as inhibitors, as well as small-molecule inhibitors that target the same pocket. These approaches will increase the likelihood that the overall effort produces cell-penetrant, reasonably potent antagonists of EH domain-dependent vesicle trafficking pathways. Ultimately, cNPF1 and related EHD1 inhibitors will allow pharmacological investigation of EHD1's roles in vesicle trafficking and its importance in cancer invasion and metastasis.

■ ASSOCIATED CONTENT

Ⓢ Supporting Information

Procedures for peptide synthesis, protein preparation, FP assays, and NMR experiments, Figures S1−S6, and Tables S1−S7. This material is available free of charge via the Internet at http://pubs.acs.org.

■ AUTHOR INFORMATION

Corresponding Author
*E-mail: joshua.kritzer@tufts.edu.

Notes
The authors declare no competing financial interests.

■ REFERENCES

(1) Mosesson, Y., Mills, G. B., and Yarden, Y. (2008) *Nat. Rev. Cancer* 8, 835−850.
(2) Caswell, P., and Norman, J. (2008) *Trends Cell Biol.* 18, 257−263.
(3) Desgrosellier, J. S., and Cheresh, D. A. (2010) *Nat. Rev. Cancer* 10, 9−22.
(4) Drakakaki, G., Robert, S., Szatmari, A. M., Brown, M. Q., Nagawa, S., Van Damme, D., Leonard, M., Yang, Z., Girke, T., Schmid, S. L., Russinova, E., Friml, J., Raikhel, N. V., and Hicks, G. R. (2011) *Proc. Natl. Acad. Sci. U.S.A.* 108, 17850−17855.
(5) Nieland, T. J., Feng, Y., Brown, J. X., Chuang, T. D., Buckett, P. D., Wang, J., Xie, X. S., McGraw, T. E., Kirchhausen, T., and Wessling-Resnick, M. (2004) *Traffic* 5, 478−492.
(6) Naslavsky, N., and Caplan, S. (2011) *Trends Cell Biol.* 21, 122−131.
(7) Jović, M., Naslavsky, N., Rapaport, D., Horowitz, M., and Caplan, S. (2007) *J. Cell Sci.* 120, 802−814.
(8) Miliaras, N. B., and Wendland, B. (2004) *Cell Biochem. Biophys.* 41, 295−318.
(9) de Beer, T., Carter, R. E., Lobel-Rice, K. E., Sorkin, A., and Overduin, M. (1998) *Science* 281, 1357−1360.
(10) Kieken, F., Jovic, M., Tonelli, M., Naslavsky, N., Caplan, S., and Sorgen, P. L. (2009) *Protein Sci.* 18, 2471−2479.
(11) de Beer, T., Hoofnagle, A. N., Enmon, J. L., Bowers, R. C., Yamabhai, M., Kay, B. K., and Overduin, M. (2000) *Nat. Struct. Biol.* 7, 1018−1022.
(12) Sharma, M., Giridharan, S. S., Rahajeng, J., Naslavsky, N., and Caplan, S. (2009) *Mol. Biol. Cell* 20, 5181−5194.
(13) Naslavsky, N., Boehm, M., Backlund, P. S., Jr., and Caplan, S. (2004) *Mol. Biol. Cell* 15, 2410−2422.
(14) Paoluzi, S., Castagnoli, L., Lauro, I., Salcini, A. E., Coda, L., Fre, S., Confalonieri, S., Pelicci, P. G., Di Fiore, P. P., and Cesareni, G. (1998) *EMBO J.* 17, 6541−6550.
(15) Salcini, A. E., Confalonieri, S., Doria, M., Santolini, E., Tassi, E., Minenkova, O., Cesareni, G., Pelicci, P. G., and Di Fiore, P. P. (1997) *Genes Dev.* 11, 2239−2249.
(16) Henry, G. D., Corrigan, D. J., Dineen, J. V., and Baleja, J. D. (2010) *Biochemistry* 49, 3381−3392.
(17) Kieken, F., Sharma, M., Jović, M., Giridharan, S. S. P., Naslavsky, N., Caplan, S., and Sorgen, P. L. (2010) *J. Biol. Chem.* 285, 8687−8694.
(18) Macia, E., Ehrlich, M., Boucrot, E., Brunner, C., and Kirchhausen, T. (2006) *Dev. Cell* 10, 839−850.
(19) Kirchhausen, T., Macia, E., and Pelish, H. E. (2008) *Methods Enzymol.* 438, 77−93.